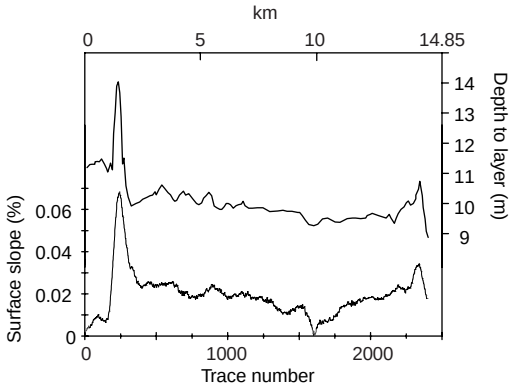

Figure 5 Comparison of accumulation rate with surface slope. The depth to a prominent internal horizon in Fig. 2b is taken as a proxy of accumulation rate. This depth is a good match to the magnitude of surface slope smoothed with a 120-m filter. Cross-correlation suggests that a 7% surface slope produces an accumulation rate ~30% higher than the regional average.

summit of Greenland was not supported by radar data[21,22]. The arches presented here are, to our knowledge, the first to be reported in the near-surface layers, at the divide, and the first to be shown to result from anomalous strain rate. We note that the width of these arches (1,570 ± 50 m) is approximately three times the ice thickness, which constitutes good agreement with Raymond's scaling analysis. The locus joining the crest of the arches tilts at −40° to the vertical, a probable indication of migration (0.5 m yr^{-1}) of the ice divide towards Rutford Ice Stream.

Although some benefits arise from collecting ice cores at ice divides, there are now at least two reasons to be wary of such sites; first, preferential wind-scouring which distorts isotopic ratios[23] and accumulation rates, and second, the possible presence of Raymond bumps. One precaution would be to ensure that flow models predicting depth–age relationships also reproduce the patterns in isochronous layers. Failure to account for Raymond bumps could incur substantial errors in accumulation-rate histories; for example, a hypothetical 100-m ice core from the crest of Fletcher Promontory would, unless corrected, yield erroneously low accumulation rates; an error of −2.6% at 10 m depth, −8% at 30 m and −26% at 100 m.

It is not yet clear over what length-scales and under what temperature conditions Raymond bumps form. But the presence of such bumps on Fletcher Promontory is a clear illustration of the nonlinear rheology of ice in a natural setting, which has often been questioned[24,25], and shows that special conditions can prevail beneath ice divides which should not be ignored when analysing even short ice cores. □

Received 16 April 1998; accepted 7 January 1999.

1. Robin, G. de Q. *The Climatic Record in Polar Ice Sheets* (Cambridge Univ. Press, 1983).
2. Clarke, T. S. & Bentley, C. R. High-resolution radar on Ice Stream B2, Antarctica: measurements of electromagnetic wave speed in firn and strain history from buried crevasses. *Ann. Glaciol.* **20,** 153–159 (1994).
3. Kohler, J., Moore, J., Kenet, M., Engeset, R. & Elvehøy, H. Using ground-penetrating radar to image previous year's summer surfaces for mass balance measurements. *Ann. Glaciol.* **24,** 255–260 (1997).
4. Raymond, C. F. Deformation in the vicinity of ice divides. *J. Glaciol.* **29,** 357–373 (1983).
5. Frolich, R. M. & Doake, C. S. M. SAR interferometry over Rutford Ice Stream and Carlson Inlet, Antarctica. *J. Glaciol.* **44,** 77–92 (1998).
6. Paren, J. G. & Robin, G. de Q. Internal reflections in polar ice sheets. *J. Glaciol.* **14,** 251–259 (1975).
7. Miners, W. D. *et al.* Forward modelling of the internal layers in radio echo sounding using electrical and density measurements from ice cores. *J. Phys. Chem. B* **101,** 6201–6204 (1997).
8. Harrison, C. H. Radio echo sounding of horizontal layers in ice. *J. Glaciol.* **12,** 383–397 (1973).
9. Black, H. P. & Budd, W. Accumulation in the region of Wilkes Land, Antarctica. *J. Glaciol.* **5,** 3–15 (1964).
10. Whillans, I. M. Effect of inversion winds on topographic detail and mass balance on inland ice sheets. *J. Glaciol.* **14,** 85–90 (1975).
11. Thomas, R. H., Stephenson, S. N., Bindschadler, R. A., Shabtaie, S. & Bentley, C. R. Thinning and grounding line retreat on the Ross Ice Shelf, Antarctica. *Ann. Glaciol.* **11,** 165–172 (1988).
12. Vaughan, D. G. Relating the occurrence of crevasses to surface strain rates. *J. Glaciol.* **39,** 255–267 (1993).
13. Dahl-Jensen, D. Two-dimensional thermo-mechanical modelling of flow and depth-age profiles near the ice divide in Central Greenland. *Ann. Glaciol.* **12,** 31–36 (1989).
14. Schøtt Hvidberg, C. Steady-state thermomechanical modelling of ice flow near the centre of large ice sheets with the finite-element technique. *Ann. Glaciol.* **23,** 116–123 (1996).
15. Weertman, J. Sliding-no sliding zone effect and age determination of ice cores. *Quat. Res.* **6,** 203–207 (1976).
16. Sandhäger, H. *Review of the Münster Airborne Radio-echo Sounding-data Set: Marine Ice beneath Filchner-Schelfeis; Bottom Reflectivity and Internal Structures of Berkner Island* 111–114 (Filchner-Ronne Ice Shelf Programe Rep. No. 9, Alfred-Wegener Inst., Bremerhaven, 1996).
17. Steinhage, D. & Blindow, N. *Results of Short Pulse Radio Echo Sounding on Thyssenhöhe, Berkner Island, Antarctica* 106–109 (Filchner-Ronne Ice Shelf Programme Rep. No. 10, Alfred-Wegener Inst. Bremerhaven, 1997).
18. Raymond, C. F. *et al.* Geometry and stratigraphy of Siple Dome, Antarctica. *Antarct. J. US* **30,** 91–93 (1995).
19. Nereson, N. A., Raymond, C. F., Waddington, E. D. & Jacobel, R. W. Recent migration of the Siple Dome ice divide, West Antarctica. *J. Glaciol.* **44,** 643–652 (1998).
20. Schøtt, C., Waddington, E. D. & Raymond, C. F. Predicted time-scales for GISP2 and GRIP boreholes at Summit, Greenland. *J. Glaciol.* **38,** 162–168 (1992).
21. Hempel, L. & Thyssen, F. Deep radio echo soundings in the vicinity of GRIP and GISP2 drill sites, Greenland. *Polarforschung* **62,** 11–16 (1992).
22. Jacobel, R. W. & Hodge, S. M. Radar internal layers from the Greenland summit. *Geophys Res. Lett.* **22,** 587–590 (1995).
23. Fisher, D. A. *et al.* Effect of wind scouring on climatic records from ice-core oxygen-isotope profiles. *Nature* **301,** 205–209 (1983).
24. Doake, C. S. M. & Wolff, W. W. Flow law for ice in polar ice sheets. *Nature* **314,** 255–257 (1985).
25. Wolff, E. W. & Doake, C. S. M. Implications of the form of the flow law for a vertical velocity and age-depth profiles in polar ice. *J. Glaciol.* **32,** 366–370 (1986).
26. Frolich, R. M., Vaughan, D. G. & Doake, C. S. M. Flow of Rutford Ice Stream and comparison to Carlson Inlet, Antarctica. *Ann. Glaciol.* **12,** 51–56 (1989).
27. Paterson, W. S. B. *The Physics of Glaciers* 3rd edn (Elsevier Science, Oxford, 1994).

Supplementary information is available on *Nature*'s World-Wide Web site and as paper copy from the London editorial office of *Nature*.

Acknowledgements. We thank C. Raymond, R. C. A. Hindmarsh, N. Nereson and colleagues at the British Antarctic Survey for their help and comments.

Correspondence and requests for materials should be addressed to D.G.V. (e-mail: d.vaughan@bas.ac.uk).

A Chinese triconodont mammal and mosaic evolution of the mammalian skeleton

Ji Qiang*†, Luo Zhexi‡ & Ji Shu-an*

** National Geological Museum of China, Beijing 100034, China*
† China University of Geosciences, Beijing 100083, China
‡ Section of Vertebrate Paleontology, Carnegie Museum of Natural History, Pittsburgh, Pennsylvania 15213-4080, USA

Here we describe a new triconodont mammal from the Late Jurassic/Early Cretaceous period of Liaoning, China. This new mammal is represented by the best-preserved skeleton known so far for triconodonts which form one of the earliest Mesozoic mammalian groups with high diversity. The postcranial skeleton of this new triconodont shows a mosaic of characters, including a primitive pelvic girdle and hindlimb but a very derived pectoral girdle that is closely comparable to those of derived therians. Given the basal position of this taxon in mammalian phylogeny, its derived pectoral girdle indicates that homoplasies (similarities resulting from independent evolution among unrelated lineages) are as common in the postcranial skeleton as they are in the skull and dentition in the evolution of Mesozoic mammals. Limb structures of the new triconodont indicate that it was probably a ground-dwelling animal.

Class Mammalia
Infraclass Triconodonta (McKenna and Bell 1997)
Order Eutriconodonta (Kermack *et al.* 1973)
Family *Incertae sedis*
Jeholodens jenkinsi gen. et sp. nov.

Etymology. Jehol: an ancient geographic name for the western part of the Liaoning Province, China; the namesake of the Jehol fauna in the Yixian Formation that yielded the holotype; *odens* (Latin): tooth; *jenkinsi* (Latin): in honour of F. A. Jenkins Jr for his pioneer studies of the evolutionary morphology of the mammalian post-cranial skeleton.

Holotype. GMV 2139 a, b, a nearly complete skeleton consisting of a partial skull and all of the postcranial skeleton preserved as two

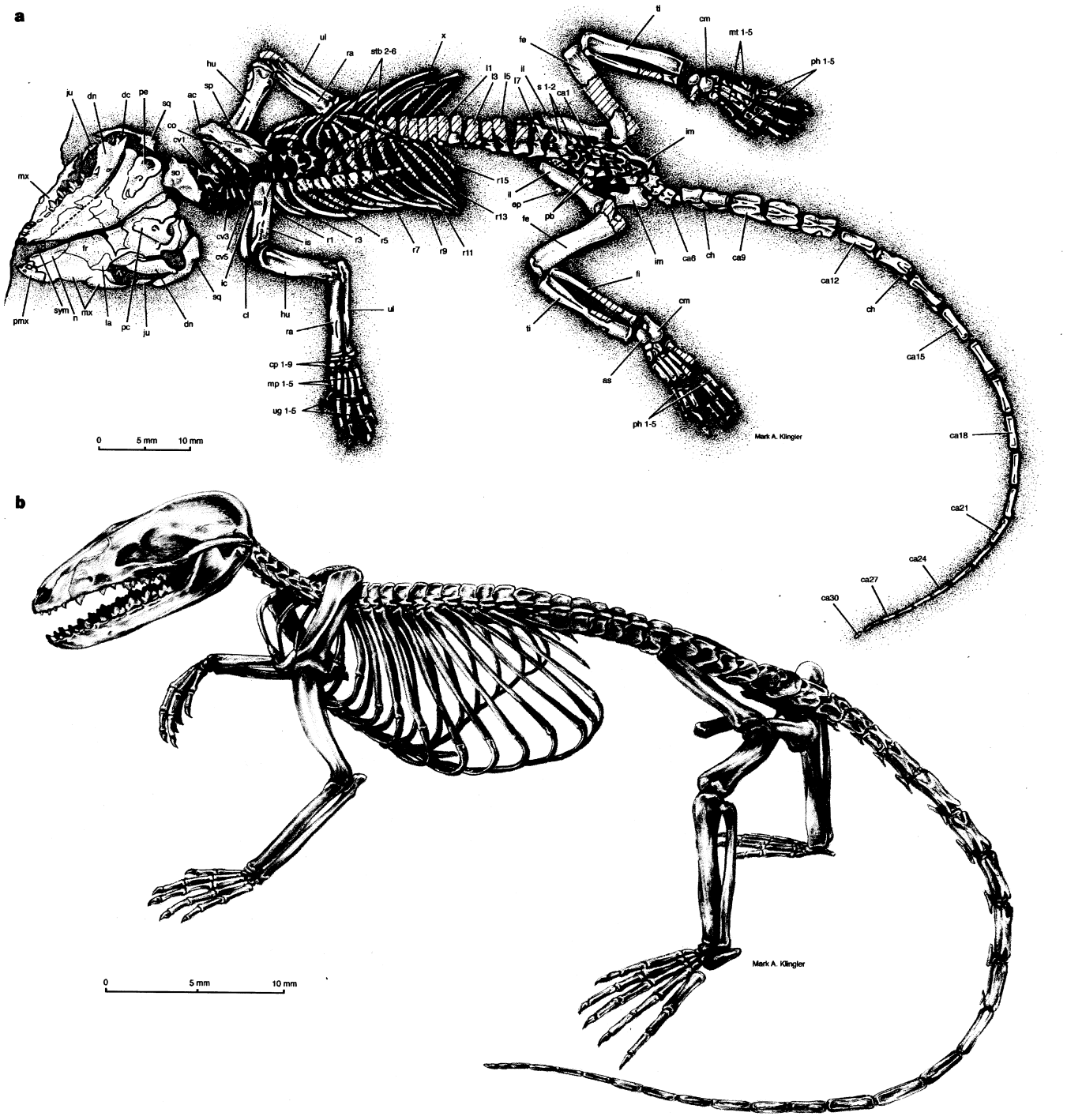

Figure 1 *Jeholodens jenkinsi* (National Geological Museum of China, holotype GMV 2139a). **a**, Dorsal view of the dorsoventrally compressed skeleton (dashed lines indicate impressions, for which the bone structures are almost completely preserved on the counterpart GMV 2139b, not shown). **b**, Reconstruction of *J. jenkinsi* as a ground-dwelling animal that had a plantigrade gait, sprawling hindlimbs and a mobile pectoral girdle with relatively wide range of excursion of the scapula but a sprawling elbow. Abbreviations: ac, acromion of scapula; as, astragalus; c, canine; c1–c7, cervical vertebrae 1–7; ca1–ca30, caudal vertebrae 1–30; ch, chevron (hemal arch); cl, clavicle; cm, calcaneum; co, coracoid process of scapula (or the unfused coracoid in cynodonts); cp1–cp9, carpals 1–9; dc, dentary condyle; dn, dentary; ep, epipubis; fe, femur; fi, fibula; fr, frontal; gl, glenoid of the scapula; hu, humerus; ic, interclavicle; il, ilium; im, ischium; is, infraspinous fossa (of scapula); i1–i4, incisors 1–4; i2r, replacement incisor 2; ju, jugal; la, lacrimal; L1–L7, lumbar vertebrae 1–7; ma, metacromion (on the spine of the scapula); mf, mandibular foramen; mg, meckelian groove; m1–4, molars 1–4; mp1–5, metacarpals 1–5; mt1–mt5, metatarsals 1–5; mx, maxillary; n, nasal; pb, pubic; pc, pars cochlearis of petrosal; pcd, coronoid process of dentary; pe, petrosal, preserved in the dorsal/endocranial view; pf, pterygoid fossa; ph1–5; phalanges 1–5; pmx, premaxillary; ps, pterygoid shelf on the ventral border of the mandible; p1, p2, premolars 1, 2; ra, radius; r1–r15, thoracic ribs 1–15; sc, scapula; sn, scapular notch; so, supraoccipital; sp, spine of scapula; sq, squamosal; ss, supraspinous fossa of scapula; stb2–6, sternebrae 2–6 (the interclavicle, the sternal manubrium and sternebra 1 are preserved and exposed by preparation, but are not shown in **a**); sym, mandibula symphysis; s1, s2, sacral vertebrae 1, 2; ti, tibia; tm, teres major fossa (on scapula); t1–t15, thoracic vertebrae 1–15; ug1–5, ungual phalanges 1–5; ul, ulna; x, xiphoid process of sternum.

counterparts (Fig. 1a; a reconstruction of the specimen is shown in Fig. 1b).

Locality and horizon. The Sihetun site (at roughly 41° 40′ 12″ N, 120° 47′ 36″ E), about 32 km east of Chaoyang City, Liaoning Province, China. The holotype is from the lacustrine shales that are intercalated with neutrobasic volcanic beds in the Yixian Formation.

Geological age and fauna. Correlation of the Yixian Formation is equivocal. It has been suggested to be Late Jurassic[1], near the Jurassic–Cretaceous boundary[2–4], or Early Cretaceous[5]. The associated fauna includes the theropods *Sinosauropteryx*[1,4], *Protarchaeopteryx*[5], *Caudipteryx*[5], the birds *Confusiusornis* and *Liaoningornis*[2], the pterosaur *Eosipterus*, the mammal *Zhangheotherium*[3], and diverse fossil fishes, invertebrates and plants.

Diagnosis. Dental formula 4·1·2·3/4·1·2·4 (incisors, canine, premolars, molars); linguobuccally compressed molars with three main cusps in a straight alignment (Fig. 2a, b); uniquely derived among triconodonts in possessing spoon-shaped incisors (Fig. 2c). *Jeholodens jenkinsi* differs from morganucodontids in lacking the molar-interlocking mechanism (by cingular cuspule e and cusp b) found in morganucodontids[6–8], in having weak labial cingula of the upper molars (Fig. 2a), in lacking lower cingular cuspules e, f and g (kuhneocone), and in lacking the angular process and the postdentary trough on the mandible (Fig. 2c). In *J. jenkinsi*, lower molar cusp a occludes into the valley-groove between cusps A and B of the opposite upper molar, thus differing from amphilestids and gobiconodontids[9,10], in which lower cusp a occludes into the embrasure anterior to upper cusp B. *J. jenkinsi* also lacks cingular cuspules e and f in the lower molars of the latter groups. The lower molars are interlocked, with a crescent-shaped distal cusp d of the preceding molar fitted into the concave mesial margin of cusp b of the succeeding molar, which is diagnostic of the Triconodontidae[11–14]. The main cusp, a, of the new taxon is much higher than cusps b and c, a primitive character that is absent in triconodontids[11–15]. *J. jenkinsi* differs from most triconodontids, other than *Alticonodon*[11] and *Ichthyoconodon*[14], in lacking the continuous lingual cingulum on the lower molars; it differs from *Alticonodon* and *Ichthyoconodon* in having a shelf-like cusp d.

Lower incisor i_2 is about to be replaced by an erupting tooth (labelled i2r in Fig. 2c) and m_4 is erupting in the holotype of *Jeholodens jenkinsi*. This dental replacement indicates that the individual probably had not reached a full adult stage. We interpret the cusp pattern and the occlusion of laterally compressed molars in *J. jenkinsi* to be indicative of an insectivorous diet.

A noteworthy skeletal feature of this new taxon is a highly derived scapula (Figs 1a, 3a), confirming an earlier observation of a triconodontid from the Cretaceous of Montana[12]. It has a robust, peg-like acromion and a low elevation on the spine that resembles the metacromion of *Didelphis* (Fig. 3f); the supraspinous fossa is fully developed. The dorsal part of the scapula has a prominent triangular area (Figs 1 and 3), similar to the large attachment area for the teres major muscle in monotremes[16], a condition also present in the archaic therian *Zhangheotherium*[3]. The clavicle is curved. Its lateral end has a tapering point with a reduced contact to the acromion, whereas in living monotremes the two structures have a rigid and broad articulation. This suggests that *Jeholodens* had a mobile scapuloclavicular articulation. Medially, the clavicle has a limited overlap with the lateral process of the interclavicle, and lacks the rigid claviculointerclavicle articulation found in the tritylodont reptiles[16] and monotremes[17]. We interpret this joint to have had at least some degree of mobility, like the conditions in multituberculates[18–20] and in archaic[3] and living[21] therians.

The distal end of the humerus bears the radial and ulnar condyles on its anterior aspect, an incipient ulnar trochlea on its posteroventral aspect, and reduced ectepicondyles and entepicondyles (on the counterpart slab; not shown), like the condition in *Zhangheotherium*[3]. These features differ from the primitive condition in cynodonts[22], morganucodontids[23], multituberculates[18–20]

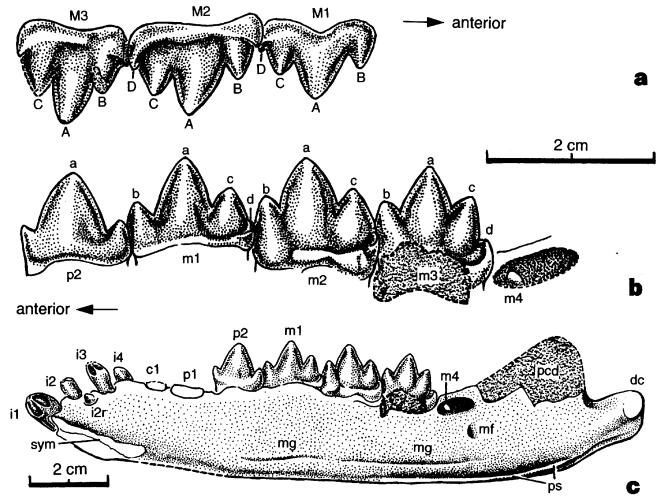

Figure 2 Dentition and mandible of *J. jenkinsi*. **a**, Upper molars M^{1-3} (right side labial view). **b**, Lower postcanines p_2–m_4 (right side, lingual view; m_4 is in the process of eruption). **c**, Mandible (right side, lingual view, corrected for slight distortion in the original specimen). Upper molars are labelled in the figure as M1–M3. Lower teeth are labelled as m1–m4; p1, p2, i1–i4 and i2r. We follow ref. 7 for the designation of cusps A–D on the upper molars and cusps a–d on the lowers. For other abbreviations see Fig. 1 legend. An analysis of mandibular and dental characters is found in Supplementary Information.

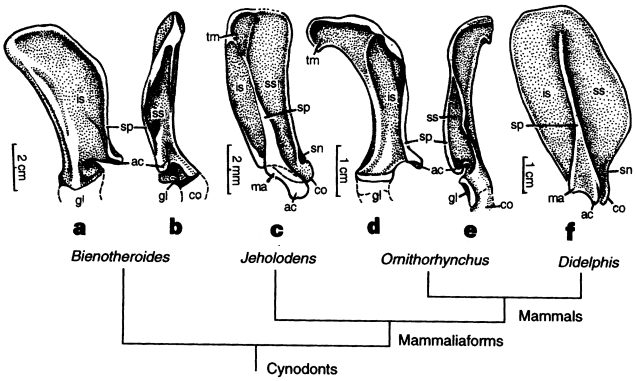

Figure 3 Mosaic evolution of the scapular characters in non-mammalian cynodonts and major mammalian clades. **a**, **b**, The tritylodontid *Bienotheroides* (lateral and anterior views of right scapula, after ref. 16, representing the outgroup condition of cynodonts[22]. **c**, *J. jenkinsi* (lateral view, right scapula, composite reconstruction from both left and right scapulae of holotype GMV 2139 a). **d**, **e**, The monotreme *Ornithorhynchus* (Carnegie Museum specimen CM 1478; lateral and anterior views of right scapula). **f**, The marsupial *Didelphis* (lateral view, right scapula). For abbreviations, see Fig. 1 legend. Given the phylogeny in Fig. 5 and those of other references[3,27], the following derived characters of the pectoral girdle and forelimb of *J. jenkinsi* and therian mammals (including *Zhangheotherium*) would be best interpreted as convergences: a full supraspinous fossa; a protruding and laterally positioned acromion; coracoid fused to scapula; a ventral and uniformly concave scapular glenoid; mobile claviculoscapular and clavicle–interclavicle joints; a greatly reduced interclavicle; reduced ectepicondyles and entepicondyles of humerus; an incipient trochlea of humerus for the ulna. Alternatively, if the features of *J. jenkinsi* and therians are regarded as primitive for mammaliaforms as a whole, then those similarities between *Ornithorhynchus* and the outgroup tritylodonts would have to be interpreted as atavistic reversals in *Ornithorhynchus* to those of cynodonts; such features include: weak supraspinous fossa on the anterior aspect of scapula; acromion on the anterior margin of scapula; a lateral and saddle-shaped glenoid; and rigid and broad articulations of the clavicle–interclavicle and the scapula–clavicle. In either scenario, homoplasies are prominent in features of the pectoral girdles and forelimbs[8,19,22]. Clade ranks following ref. 27; see also the alternatives given in refs 8, 29.

and living monotremes, in which the humerus has no ulnar trochlea. The epiphyseal suture is not present in the long bones in the holotype of *J. jenkinsi*.

In contrast to the derived forelimb and pectoral girdle of *Jeholodens jenkinsi*, its pelvic girdle, hindlimb and pes share many plesiomorphic characters with morganucodontids[23], tritylodontids[16] and other cynodonts[22]. The epipubis is present. The patellar groove on the distal femur is far less developed than in monotremes, multituberculates and therians. The calcaneum (Fig. 4b) has a very short tubercle, a broad anterolateral ('peroneal') shelf, and extensive fibular and tibial facets, all of which are identical to those of morganucodontids[23] and non-mammalian cynodonts[22], but different from the distinct peroneal process in monotremes, multituberculates[18,19] and therians[24] and from the elongate tubercle of multituberculates and therians. The astragalus has a broad and uniformly convex tibial facet, but a weakly developed neck and navicular facet. The astragalus and calcaneum contact each other in juxtaposition; this condition is similar to that in non-mammalian cynodonts[22] and morganucodontids[23], but different from the partial overlap of these two ankle bones in multituberculates and the complete overlap of these bones in archaic[24] and living therians (Fig. 4). Metatarsal 5 is offset from the cuboid (Fig. 4), allowing a wide range of abduction of the lateral pedal digits, as in morganucodontids[23], monotremes and multituberculates[19]. The manual and pedal ungual phalanges are slightly curved dorsally and concave on both sides, similar to those of most ground-dwelling small mammals[19,25]. A flexor tubercle on the midpoint in most of the ungual phalanges indicates a certain degree of ability to flex the claws. *J. jenkinsi* lacks the sesamoid ossicle(s) of the monotremes, multituberculates and therians. We interpret *J. jenkinsi* to have been a ground-dwelling small mammal with a plantigrade gait (Fig. 1b) and some capability for climbing on uneven substrates[23], but not an arboreal mammal.

The eutriconodonts first appeared in the Middle Jurassic[15] and were quite diverse, with a worldwide distribution, in the Cretaceous[9–14]. Although abundantly represented by teeth[9–15] and some cranial[12,15,26] and postcranial[9] materials, no fully articulated skeleton was known, until now, for this diverse group. In traditional classifications of early mammals that were based primarily on dentition[6,12,15], eutriconodonts and morganucodontids belonged to the order Triconodonta. The traditional grouping of 'triconodonts' (morganucodontids + eutriconodonts) is considered to be a grade, rather than a monophyletic group, according to more recent phylogenetic analyses[26–28]. Studies of some dental and cranial characters indicate that eutriconodonts may also be a heterogeneous group[10,28].

It has been proposed that the postcranial features of cynodonts and early mammals were subjected to functional constraints of locomotion and therefore susceptible to homoplasies[19,22,29]. Several cladistic studies of cynodonts and early mammals that incorporated postcranial characters[27,30] indicated that dental characters are highly homoplastic, whereas the postcranial characters can be very informative for higher-level phylogeny. Because of the paucity of the relatively complete postcrania of the basal mammals, it is unknown whether (or to what degree) homoplasies exist among different postcranial skeletal parts (such as the forelimb versus the hindlimb) in early mammalian evolution.

The discovery of the first fully articulated triconodont skeleton offers an unprecedented opportunity for a more comprehensive assessment of the relationships of triconodonts, combining all evidence of the dentition, basicranium and postcranium, and will also allow us to elucidate the pattern of postcranial evolution in early mammals. Our phylogenetic analysis has placed *J. jenkinsi* in the basal part of the mammalian phylogenetic tree, outside the crown group of extant Mammalia (Fig. 5). Available evidence indicates that *J. jenkinsi* is a eutriconodont and far more derived than morganucodontids. Within eutriconodonts, the new taxon is more closely related to the triconodontid clade than it is to amphilestids and gobiconodontids (see Supplementary Information). These results are consistent with the ideas that triconodonts are paraphyletic[26–28] and that the triconodont-like molar cusp and occlusal patterns are characters for a functional grade.

Jeholodens jenkinsi shows a mosaic of derived, therian-like characters for most parts of the pectoral girdle (Fig. 3) and the humerus, but very primitive characters for the vertebral column, pelvic girdle, hindlimb and pes (Fig. 4). Our phylogenetic analysis indicates that many apomorphies of the pectoral girdle and forelimb in *J. jenkinsi* are independently derived and convergent with those of therians. Such apomorphies include a fully developed supraspinous fossa, the acromion and metacromion on the scapular spine, the incipient ulnar trochlea and the reduced epicondyles of the humerus. Given the phylogeny shown in Fig. 5, the mobile clavicle and scapula in *J. jenkinsi* would represent convergences with those of the multituberculate–therian clade[3,20,27]. Thus these pectoral

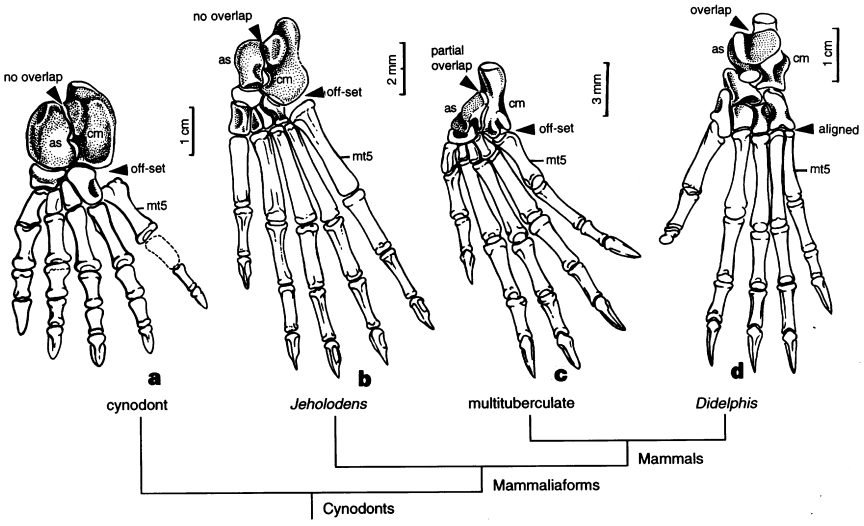

Figure 4 Pedes of mammals and outgroup cynodonts. **a**, A generalized cynodont condition (after refs 22, 28). **b**, *J. jenkinsi* (composite reconstruction of holotype GMV 2139 a,b). **c**, The multituberculate *Eucosmodon* (after refs 18, 19). **d**, The therian *Didelphis*. *J. jenkinsi* has little or no overlap of the astragalus and calcaneum, a primitive feature of cynodonts, contrasting with the partial overlap of these characters in multituberculates and the complete overlap in therians. Clade ranks follow ref. 27; see also the alternatives given in refs 8, 29.

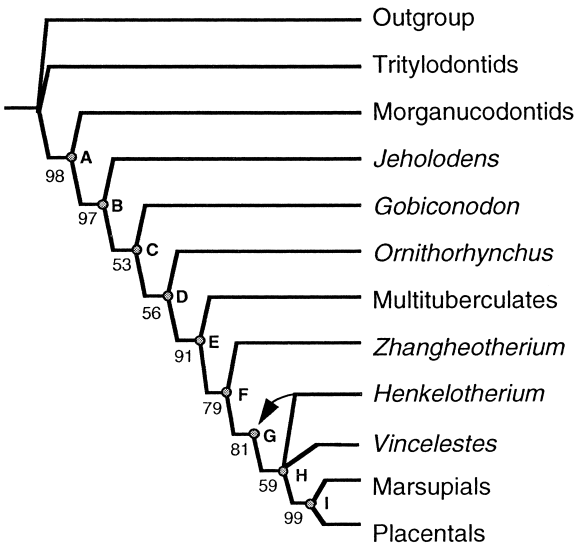

Figure 5 Evolutionary relationships of *J. jenkinsi*, gen. et sp. nov. The derived characters related to a mobile pectoral girdle occur separately on nodes B and E. The 'primitive' characters related to an immobile pectoral girdle occur in tritylodontids and the cynodont outgroup, and separately in *Ornithorhynchus* (node D). This indicates that there are many homoplasies of pectoral girdles and forelimbs (in contrast to the few or no convergences in the pelvic girdle and hindlimb), given the same tree topology of major clades of mammals. The arrow indicates an alternative placement of *Henkelotherium* at node G. For details of phylogenetic analysis see Methods and Supplementary Information.

characters, which allow a greater range of excursion of the shoulder joint in the locomotion of multituberculates[3,19,20] and living therians[21], have evolved at least twice among the Mesozoic mammals.

Alternatively, the mobile joints between the clavicle, interclavicle and scapula could be ancestral conditions shared by *J. jenkinsi* and the more derived mammals. If so, then the rigid clavicle–interclavicle articulation and relatively immobile scapula of monotremes (Fig. 3) would have to be regarded as atavistic reversals to the primitive conditions in the more distantly related non-mammalian cynodonts[16,22]. For either evolutionary scenario, we must conclude that the pectoral girdles and forelimbs of early mammals underwent extensive convergent evolution, not only by comparison with the dental and cranial features, but also in relation to more conservative features of the pelvis and hindlimbs. □

Methods

Phylogeny of mammals (Fig. 5) is based on a strict consensus of two equally parsimonious trees (tree length = 210; consistency index = 0.638; retention index = 0.724) from PAUP analysis (3.1.1. Branch and Bound search) of 101 dental, cranial and postcranial characters that can be scored for the 12 major clades of mammals (see Supplementary Information). Most of the characters are preserved in the holotype of *Jeholodens jenkinsi*. The two most pasimonious trees differ only in the alternative placements of *Henkelotherium*, which either is at node G (represented by an arrow in Fig. 5) or switches positions with *Vincelestes*. These alternative placements of *Henkelotherium* do not alter the positions of any other clades, including *J. jenkinsi*. Numbers on branches represent the percentage of bootstrap values in 1,000 bootstrap replicas for a 50% majority bootstrap consensus tree that has identical topology to one of the two most parsimonious trees (that in which *Henkelotherium* is positioned at node G).

Received 26 August 1998; accepted 27 January 1999.

1. Ji, Q. & Ji, S.-A. Discovery of the earliest bird fossils in China and the origin of birds. *Chinese Geol.* **1996,** 30–33 (1996).
2. Hou, L., Martin, L. D., Zhou, Z. & Feduccia, A. Early adaptive radiation of birds: evidence from fossils from Northeastern China. *Science* **274,** 1164–1165 (1996).
3. Hu, Y., Wang, Y., Luo, Z. & Li, C. A new symmetrodont mammal from China and its implications for mammalian evolution. *Nature* **390,** 137–142 (1997).
4. Chen, P.-J., Dong, Z.-M. & Zhen, S.-N. An exceptionally well-preserved theropod dinosaur from the Yixian Formation of China. *Nature* **391,** 147–152 (1998).
5. Ji, Q., Currie, P. J., Norell, M. A. & Ji, S.-A. Two feathered dinosaurs from northeastern China. *Nature* **393,** 753–761 (1998).
6. Kermack, K. A., Mussett, F. & Rigney, H. W. The lower jaw of *Morganucodon*. *Zool. J. Linn. Soc.* **53,** 87–175 (1973).
7. Crompton, A. W. The dentitions and relationships of the southern African Triassic mammals *Erythrotherium parringtoni* and *Megazostrodon rudnerae*. *Bull. Br. Mus. Nat. Hist.* **24,** 399–437 (1974).
8. Luo, Z. in *In the Shadow of Dinosaurs—Early Mesozoic Tetrapods* (eds Fraser, N. C. & Sues, H.-D.) 980–128 (Cambridge Univ. Press, Cambridge, 1994).
9. Jenkins, F. A. Jr & Schaff, C. R. The Early Cretaceous mammal *Gobiconodon* (Mammalia, Triconodonta) from the Cloverly Formation in Montana. *J. Vert. Paleontol.* **6,** 1–24 (1988).
10. Kielan-Jaworowska, Z. & Dashzeveg, D. New Early Cretaceous amphilestid ('triconodont') mammals from Mongolia. *Acta Palaeont. Polonica.* **43,** 413–438 (1998).
11. Fox, R. C. Additions to the mammalian local fauna from the upper Milk River Formation (Upper Cretaceous), Alberta. *Can. J. Earth Sci.* **13,** 1105–1118 (1976).
12. Jenkins, F. A. Jr & Crompton, A. W. in *Mesozoic Mammals: The First Two-thirds of Mammalian History* (eds Lillegraven, J. A., Kielan-Jaworowska, Z. & Clemens, W. A.) 74–90 (Univ. Calif. Press, Berkeley, 1979).
13. Cifelli, R. L., Wible, J. R. & Jenkins, F. A. Jr Triconodont mammals from the Cloverly Formation (Lower Cretaceous), Montana and Wyoming. *J. Vert. Paleontol.* **16,** 237–241 (1998).
14. Sigogneau-Russell, D. Two possibly aquatic triconodont mammals from the Early Cretaceous of Morocco. *Acta Palaeont. Polonica* **40,** 149–162 (1995).
15. Simpson, G. G. *A catalogue of the Mesozoic Mammalia in the Geological Department of the British Museum* (Oxford Univ. Press, London, 1928).
16. Sun, A. & Li, Y. The postcranial skeleton of the late tritylodont *Bienotheroides*. *Vert. PalAsiat.* **23,** 136–151 (1985).
17. Klima, M. Die Frühentwicklung des Schültergürtels und des Brustbeins bei den Monotremen (Mammalia: Prototheria). *Adv. Anat. Embryol. Cell Biol.* **47,** 1–80 (1973).
18. Krause, D. W. & Jenkins, F. A. Jr The postcranial skeleton of North American multituberculates. *Bull. Mus. Comp. Zool.* **150,** 199–246 (1983).
19. Kielan-Jaworowska, Z. & Gambaryan, P. P. Postcranial anatomy and habits of Asian multituberculate mammals. *Fossils Strata* **36,** 1–92 (1994).
20. Sereno, P. & McKenna, M. C. Cretaceous multituberculate skeleton and the early evolution of the mammalian shoulder girdle. *Nature* **377,** 144–147 (1995).
21. Jenkins, F. A. Jr & Weijs, W. A. The functional anatomy of the shoulder in the Virginia opossum (*Didelphis virginiana*). *J. Zool.* **188,** 379–410 (1979).
22. Jenkins, F. A. Jr The postcranial skeleton of African cynodonts. *Bull. Peabody Mus. Nat. Hist. Yale Univ.* **36,** 1–216 (1971).
23. Jenkins, F. A. Jr & Parrington, F. R. Postcranial skeleton of the Triassic mammals *Eozostrodon*, *Megazostrodon*, and *Erythrotherium*. *Phil. Trans. R. Soc. Lond. B* **273,** 387–431 (1976).
24. Rougier, G. W. *Vincelestes neuquenianus* Bonaparte (Mammalia, Theria), un primitivo mammifero del Cretacico Inferior de la Cuenca Neuqina. Thesis, Univ. Nacional de Buenos Aires (1993).
25. McLeod, N. & Rose, K. D. Inferring locomotory behavior in Paleogene mammals via eigenshape analysis. *Am. J. Sci.* **293,** 300–355 (1993).
26. Rougier, G. W., Wible, J. R. & Hopson, J. A. Basicranial anatomy of *Priacodon fruitaensis* (Triconodontidae, Mammalia) from the Late Jurassic of Colorado, and a reappraisal of mammaliaform interrelationships. *Am. Mus. Novit.* **3183,** 1–28 (1996).
27. Rowe, T. Definition, diagnosis, and origin of Mammalia. *J. Vert. Paleontol.* **8,** 241–264 (1988).
28. Kielan-Jaworowska, Z. Characters of multituberculates neglected in phylogenetic analyses of early mammals. *Lethaia* **29,** 249–255 (1997).
29. Hopson, J. A. in *Major Features of Vertebrate Evolution* (eds Prothero, D. R. & Schoch, R. M.) 190–219 (Short Courses in Paleontol. No. 7, Paleontol. Soc. Knoxville, Tennessee, 1994).
30. Kemp, T. S. The relationships of mammals. *Zool. J. Linn. Soc.* **77,** 353–384 (1983).

Supplementary information is available on *Nature*'s World-Wide Web site (http://www.nature.com) or as paper copy from the London editorial office of *Nature*.

Acknowledgements. We thank K. C. Beard, R. L. Cifelli, W. A. Clemens, A. W. Crompton, M. R. Dawson, J. A. Hopson, F. A. Jenkins, Z. Kielan-Jaworowska, J. Meng, T. Rowe, D. Sigogneau-Russell, J. R. Wible and X.-c. Wu for discussions and for reviews of the manuscript; A. Henrici for preparation of the specimen; M. Klingler for preparing Fig. 1; and N. Wuethele for assistance. This research was supported by funding from the Ministry of Geology and Mineral Resources of China and the National Natural Science Foundation of China (to J.Q.), and the US National Science Foundation, the National Geographic Society, and the M. Graham Netting Fund of the Carnegie Museum (to Z.L.).

Correspondence and requests for materials should be addressed to: Z. Luo (e-mail: luoz@clpgh.org).

Strong effects of weak interactions in ecological communities

E. L. Berlow

Department of Integrative Biology, University of California, Berkeley, California 94720-3140, USA

The loss or removal of individual species can cause dramatic changes in communities[1–5]. Experiments indicate that in many communities only a few species will have such strong effects, whereas most will have weak effects owing to small *per capita* effects and/or low abundance[3,6–15,16]. But extinction of these 'weak' interactors could significantly alter natural communities because they play important stabilizing or 'noise-dampening' roles[14,15,17–23]. I